



HAL
open science

Antagonistic interactions between odorants alter human odor perception

Yosuke Fukutani, Masashi Abe, Haruka Saito, Ryo Eguchi, Toshiaki Tazawa, Claire A de March, Masafumi Yohda, Hiroaki Matsunami

► **To cite this version:**

Yosuke Fukutani, Masashi Abe, Haruka Saito, Ryo Eguchi, Toshiaki Tazawa, et al.. Antagonistic interactions between odorants alter human odor perception. *Current Biology - CB*, 2023, 33 (11), pp.2235-2245.e4. 10.1016/j.cub.2023.04.072 . hal-04220853

HAL Id: hal-04220853

<https://hal.science/hal-04220853>

Submitted on 28 Sep 2023

HAL is a multi-disciplinary open access archive for the deposit and dissemination of scientific research documents, whether they are published or not. The documents may come from teaching and research institutions in France or abroad, or from public or private research centers.

L'archive ouverte pluridisciplinaire **HAL**, est destinée au dépôt et à la diffusion de documents scientifiques de niveau recherche, publiés ou non, émanant des établissements d'enseignement et de recherche français ou étrangers, des laboratoires publics ou privés.

1 **Article**

2

3 **Title**

4 Antagonistic interactions between odorants alter human odor perception.

5

6 **Authors**

7 Yosuke Fukutani^{1,2,*}, Masashi Abe¹, Haruka Saito¹, Ryo Eguchi³, Toshiaki Tazawa³, Claire A.
8 de March⁴, Masafumi Yohda^{1,2,*}, Hiroaki Matsunami^{2,4,5,*}

9

10 **Affiliations**

11 ¹Department of Biotechnology and Life Science, Tokyo University of Agriculture and
12 Technology, Koganei, Tokyo 184-8588, Japan

13 ²Institute of Global Innovation Research, Tokyo University of Agriculture and Technology,
14 Koganei, Tokyo 184-8588, Japan.

15 ³Research Section, R & D Division, S.T. Corporation, Shinjuku, Tokyo 161-0033, Japan.

16 ⁴Department of Molecular Genetics and Microbiology, Duke University Medical Center,
17 Durham, North Carolina 27710.

18 ⁵Department of Neurobiology, Duke Institute for Brain Sciences, Duke University Medical
19 Center, Durham, North Carolina 27705.

20

21 *: Correspondence, Y. F. (fukutani@cc.tuat.ac.jp), M. Y. (yohda@cc.tuat.ac.jp) and H.M.
22 (hiroaki.matsunami@duke.edu)

23 **Abstract**

24 The olfactory system detects a vast number of odorants using hundreds of olfactory receptors
25 (ORs), the largest group of the G protein-coupled receptor (GPCR) superfamily. Each OR is
26 activated by specific odorous ligands. Like other GPCRs, activation of ORs may be blocked
27 through antagonism. Recent reports highlight widespread antagonisms in odor mixtures
28 influencing olfactory neuron activities. However, it is unclear if and how these antagonisms
29 influence perception of odor mixtures. Here we show that odorant antagonisms at the receptor
30 level alter odor perception. Using a large-scale heterologous expression, we first identified a set
31 of human ORs that are activated by methanethiol and hydrogen sulfide, two extremely potent
32 volatile sulfur malodors. We then screened odorants that block activation of these ORs and
33 identified a set of antagonists, including β -ionone. Finally, human sensory evaluation revealed
34 that odor intensity and unpleasantness of methanethiol were decreased by β -ionone. Odor
35 intensity of β -ionone itself is not correlated with the degree of suppression of malodor
36 sensation. Suppression was also not observed when methanethiol and β -ionone were
37 simultaneously introduced to different nostrils. Together, our data supports the model that odor
38 sensation is altered through antagonistic interactions at the level of the ORs.

39

40

41

42 **Introduction**

43 Animals detect and discriminate numerous environmental odorants through combinatorial
44 activation of membrane receptors expressed in olfactory sensory neurons (OSNs). In humans,
45 the predominant receptors are the olfactory receptors (ORs), which are the largest protein-
46 coding gene family of Class A G-protein coupled receptors (GPCRs) with ~400 members¹⁻⁵.
47 When an odorous agonist binds to an OR, the OR favors an active conformation that initiates a
48 signal transduction cascade, leading to depolarization of the OSNs. Each OSN expresses only
49 one type of OR, meaning that the activation of an OSN is determined by the activation of the
50 OR^{6,7}. A single OR can respond to various odorants, and one odorant activates multiple ORs.
51 Thus, the combinatorial pattern of OR activation is foundational for the detection and
52 discrimination of a given odor⁸⁻¹¹.

53 In addition to acting as an agonist, comparative to ligands for canonical GPCRs, some
54 odorants can function as antagonists or inverse agonists. By binding to ORs, odorants can
55 inhibit the activation by agonists in a competitive manner or stabilize the receptor in the
56 inactive conformation. Previous *in vivo* and *ex vivo* studies as well as *in vitro* research using
57 heterologously expressed ORs have shown that odorants are often capable of acting as
58 antagonists for ORs¹²⁻¹⁹. Natural odors are usually mixtures of odorants, so antagonistic
59 interactions between odorants at ORs are likely. Mixture suppression, in which odor intensity is
60 less than a linear sum of component odorants, is commonly observed^{20,21}. Previous studies
61 highlighted the role of central olfactory processing in mixture suppression²²⁻²⁴. Yet peripheral
62 events, such as antagonistic interactions of odorants at the ORs, were also proposed as an
63 underlying mechanism of mixture suppression^{24,25}. Despite widespread antagonism on OSNs in

64 odor mixtures, there is scarce evidence supporting a role of odorant antagonism in odor
65 perception^{20,26}. This is partly because OR antagonists also act as agonists for other ORs,
66 making it challenging to distinguish the role of antagonism in odor perception from central
67 processing.

68 In this study, we addressed the effects of odorant antagonism in odor perception by
69 focusing on a set of ORs that are activated by extremely potent and unpleasant volatile sulfur
70 compounds (VSCs), including methanethiol (methyl mercaptan, CH₃SH). Antagonists, such as
71 β -ionone, blocked the VSC OR response and modified the sulfur odorants odor perception.

72

73 **Results**

74 **Screening human ORs that respond to gaseous sulfur compounds**

75 Previously, we developed a method to detect *in vitro* OR responses to odors in the vapor
76 phase^{11,27}. Using this technique with modifications (see Methods), we performed an OR
77 screening assay for two highly volatile sulfur compounds (VSCs), methanethiol and hydrogen
78 sulfide (Fig. 1A and Extended data Fig. 1).

79 By screening the response of 359 human ORs, representing the vast majority of intact ORs
80 encoded on the human genome, to methanethiol and hydrogen sulfide, we identified several
81 candidate hits that exhibited strong responses ($p < 0.001$, one-way ANOVA followed by Dunnett's
82 test) (Fig. 1B and Supplementary Data). A secondary screening confirmed concentration-
83 dependent responses of OR2T11 and OR2T1 to methanethiol and hydrogen sulfide as well as
84 the response of OR2T6 to hydrogen sulfide (Fig. 1C). These three ORs share relatively high
85 amino acid sequence similarities among the OR family members (Identities; 73% (222/305),
86 66% (206/310), and 63% (193/304) in OR2T1/OR2T6, OR2T1/OR2T11, OR2T6/OR2T11,
87 respectively) (Fig. 1D).

88 OR2T11 was previously shown to respond to various thiol molecules in a copper- and silver
89 ion-dependent manner²⁸⁻³⁰. We examined the metal dependence of the ORs' responses to
90 methanethiol and hydrogen sulfide. Consistent with the previous reports, the addition of copper
91 in the media dramatically enhanced the response to both VSCs. The addition of silver produced
92 moderate response enhancement, while the addition of zinc showed no effect (Extended data
93 Fig. 2A). The effect of copper was diminished by the addition of the copper chelator
94 tetraethylenepentamine (TEPA) (Extended data Fig. 2B). Our data supports the previously

95 suggested model that metal-sulfur complexes activate sulfur-responsive ORs.

96

97 **Identification of antagonists**

98 Antagonists or inverse agonists of ORs that are potently activated by the sulfur odorants
99 may block the perception of their unpleasant odor, potentially leading to the development of
100 novel deodorants. To identify antagonists that block the activity of VSC-responding ORs, we
101 screened the effects of 100 odorants on OR2T11 response to methanethiol and hydrogen
102 sulfide. OR2T11-expressing cells in a buffer containing each compound at a final concentration
103 of 100 μ M were stimulated by 7 ppm methanethiol and 41 ppm hydrogen sulfide. A subset of
104 ketones, including specific ionones and damascones, showed inhibitory effects on the OR
105 responses against the tested VSCs (Fig. 2A). β -ionone was the most potent antagonist among
106 the tested odorants ($\text{LogIC}_{50} = -4.85$) (Fig. 2B and Extended data Fig. 3A) and did not alter the
107 activity of OR2T11 by itself when tested without VSCs (Fig. 2C). In contrast, Iso E super
108 (tetramethyl acetyloctahydronaphthalen)^{31,32}, which is one of the most commonly used ketone
109 fragrances for deodorant, did not show potent antagonistic effects on OR2T11 (Fig. 2B).

110 Next, we examined the inhibitory effects of the ionone and damascone molecules on the
111 responses of OR2T11, OR2T1, and OR2T6 to the VSCs. We observed that all tested ORs were
112 similarly inhibited by a given antagonist, suggesting a common blocking mechanism. (Fig. 2D
113 and Extended data Fig. 3B). The possibility that the inhibition of the odorants was caused by
114 adverse effects on the assay system, such as cytotoxicity, was excluded because another OR,
115 mouse Or2aj6 (also known as Olfr171 and MOR273-1), was activated by these compounds in
116 the same assay (Extended data Fig. 3C). In the vapor stimulation assays, a mixture of

117 methanethiol and β -ionone also showed a concentration-dependent and molecule-specific
118 inhibitory effect against OR2T11 and OR2T6 (Fig. 2E and Extended data Fig. 4A). Since the
119 concentration of methanethiol did not decrease by mixing with β -ionone in the sampling bag
120 (Extended data Fig. 4B), chemical reactions between methanethiol and β -ionone is unlikely to
121 be a cause of suppression of OR activations.

122 To gain insight into mechanism underlying the antagonisms, we performed docking of the
123 ligands on the structural models of OR2T families based on AlphaFold2³³ (Extended data Fig.
124 5). Following previous publications and our data suggesting copper as an essential co-factor to
125 antagonism (Extended data Fig. 2), OR bound to sulfur odorants by coordinating with a copper
126 cation at the level of sulfur residues^{28-30,34,35}. The docking of copper resulted in a binding close
127 to C^{BW5.43} and M^{BW5.39}. These residues, conserved in a small subset of ORs including OR2T1,
128 OR2T6, and OR2T11, pointed towards the odorant binding cavity (Fig. 3F and Extended data
129 Fig. 6A). The bottom of this cavity was defined by the OR toggle switch, the “FYG” motif
130 (BW6.47 to BW6.49), in the transmembrane helix (TM) 6³⁶. Hydrogen sulfide and
131 methanethiol were docked on the copper bound OR structures. All poses were located in
132 between the copper and the toggle switch (Fig 3F and Extended data Fig. 6), suggesting a
133 possibility of effective binding for these two molecules in OR2T1, OR2T6, and OR2T11. The
134 β -ionone binding location overlapped with that of the Cu-sulfur odorant in all three structures
135 when it was docked into the cavity of OR2T1, OR2T6, and OR2T11. This model is consistent
136 with the idea that β -ionone antagonizes OR activation by competitively blocking the binding of
137 Cu-sulfur odorant.

138

139 **Human sensory evaluation test**

140 Thus far, we have identified that OR2T family members robustly respond to the tested
141 VSCs and that certain ketones, including β -ionone, act as antagonists. If antagonists inhibit the
142 response of all receptors that respond to particular VSCs, it is expected that inhibition of
143 olfactory perception will occur. To test whether the antagonistic interactions affect olfactory
144 perception, we designed a set of human sensory evaluation tests aiming to distinguish
145 antagonistic effects and central processing in mixture suppression. We selected β -ionone
146 (floral/violet/woody smell), the most potent antagonist we identified, in parallel with Iso E
147 Super (woody/floral/amber/violet smell), which does not show potent antagonistic effects (Fig.
148 2B). While perceived odor intensities of β -ionone and Iso E Super varied among subjects, we
149 adjusted their concentrations so that the intensities were matched as a group (Fig. 3A and
150 Extended data Fig. 7 and 8). Iso E Super is more pleasant than β -ionone at the adjusted
151 concentrations (***) $p < 0.001$, non-parametric Wilcoxon test) (Extended data Fig. 8B). Sensory
152 evaluation tests were conducted by asking subjects to rate total odor intensity, malodor
153 intensity, and pleasantness of methanethiol and its mixtures (methanethiol and β -ionone,
154 methanethiol and Iso E Super). The subjects were separated into two groups with different
155 evaluation orders (Extended data Fig. 8C). In order to clarify the evaluation criteria for the
156 subjects, we presented the odors in a non-random order. We first conducted a non-blind test for
157 methanethiol and asked subjects to score one value for both total odor intensity and malodor
158 intensity. Subsequently, two odor mixtures (methanethiol with either β -ionone and
159 methanethiol with Iso E Super) were presented in a random order to separately evaluate total
160 odor intensity, malodor intensity, and pleasantness in the blind condition (Extended data Fig.

161 8C). Regardless of the order of odor presentation, the subjects' evaluations were similar,
162 excluding the role of odor adaptation in our tests ($p>0.05$, Mann-Whitney tests) (Extended data
163 Fig. 7B). The total odor intensity of methanethiol and β -ionone mixtures was less than those of
164 the methanethiol only, indicating mixture suppression ($p<0.001$, Wilcoxon test) (Fig. 3C Left).
165 Additionally, the malodor intensity and unpleasantness of methanethiol was significantly
166 reduced by mixing it with β -ionone ($p<0.001$, Kruskal-Wallis test) (Fig. 3C Center and Right).
167 To test whether odor intensity of β -ionone alone predicts its suppressive effects on
168 methanethiol, we first focused on the group with low odor intensity against β -ionone (6 out of
169 20 subjects) and found that the suppressing effect was evident ($p=0.03$, nonparametric
170 Wilcoxon multiple comparison test) (Fig. 3D). When we compare the suppressing effects
171 between this group and the group with higher odor intensity against β -ionone (14 out of 20
172 subjects), there was no statistically significant difference in methanethiol suppression ($p=0.98$,
173 Mann-Whitney test). Moreover, both of the odor intensities and the pleasantness of β -ionone
174 showed no significant correlation with the degree of suppressing effects against methanethiol
175 ($p=0.58$ and 0.84 , respectively, Spearman's tests) (Fig. 3E). Together, the data suggests that
176 odor intensity of β -ionone alone is independent from its odor suppressing effects. In the
177 Relative rank, mixture of β -ionone was significantly higher than one of Iso E Super in the
178 evaluation of malodor intensity ($p=0.02$, nonparametric Friedman's multiple comparison test)
179 (Fig. 3F). Iso E Super also reduced total odor intensity, malodor intensity, yet it was less
180 effective in suppressing malodor intensity than β -ionone (Fig. 3F and Extended data Fig. 8).
181 Similarly, damascones (α -damascone, β -damascone, δ -damascone) and β -damascenone that
182 inhibited OR response to the VSCs were effective in reducing the odor intensity and

183 unpleasantness to methanethiol (Extended data Fig. 9). δ -damascone, which showed a low
184 inhibitory effect in *in vitro* assay (Fig. 2D), also had the lowest suppressing effect among the
185 tested antagonists in the sensory evaluation test. Together, the data is consistent with our
186 hypothesis that antagonistic effects on ORs change odor perception.

187

188 **Nostril-specific stimulation**

189 Finally, to differentiate the impact of peripheral antagonism vs central processing in
190 the malodor suppression, we compared the impact of β -ionone on the perception of
191 methanethiol when β -ionone was inhaled via the same versus a different nostril (Fig. 4A). The
192 subjects were unable to distinguish which nostril the tested odor was presented to (Fig. 4B).
193 This is consistent with previous reports stating that humans cannot identify the directionality of
194 OSNs when OSNs are stimulated and somatosensory nerves in the nasal cavity are not³⁷. For
195 β -ionone single stimulation at the adjusted concentrations, subjects tended to evaluate that the
196 malodor intensity and pleasantness were neither strong nor weak, and those who felt a strong
197 odor evaluated the malodor intensity higher. (Fig. 4C). Despite being performed in the blind
198 test, all the subjects gave the same score for total odor intensity and malodor intensity for
199 conditions contained methanethiol (Fig. 4D and Supplementary Data). When premixed gas of
200 methanethiol and β -ionone was inhaled from one nostril, total odor intensity, malodor intensity
201 and unpleasantness was reduced with compared to that of each of the components inhaled
202 individually (* $p=0.035$, * $p=0.035$ and $p=0.031$, respectively, Kruskal-Wallis test) (Fig. 4D and
203 4E). In a striking contrast, when methanethiol and β -ionone were simultaneously inhaled
204 through different nostrils, no significant suppression effect was observed in total odor intensity,

205 malodor intensity and pleasantness ($p=0.27$, $p=0.27$ and $p=0.072$, respectively, Kruskal-Wallis
206 test) (Fig. 4D and 4E). In relative ranking, it is clear that premixed gas showed a significant
207 change in malodor intensity, and that individual stimulation did not ($*p\leq 0.05$, nonparametric
208 Friedman's multiple comparison test) (Fig. 4F). Altogether, these results suggest that
209 antagonistic effects of β -ionone on methanethiol-responsive ORs altered odor perception.

210

211 Discussion

212 OR antagonisms are hypothesized to play an essential role in odor perception, based on
213 previous reports showing widespread antagonistic interactions of odor mixtures at the level of
214 OSNs and ORs in rodents^{15,16,18,38,39} in conjunction with widespread mixture suppression of
215 odors in humans^{24,40}. This study shows that OR2T1 and OR2T11 are activated by methanethiol
216 and antagonized by β -ionone *in vitro*. This corroborates our psychophysics studies showing that
217 β -ionone reduces the intensity and unpleasantness of methanethiol in mixtures. Our results
218 imply that activation of specific OR2T members by certain VSCs induces a characteristic foul
219 odor sensation. Blocking OR2T activation using specific ketone antagonists, such as β -ionone,
220 results in lower odor intensity and unpleasantness of the VSCs, which suggests that OR
221 antagonism plays a prominent role in odor perception

222 Previous studies show that genetic variations of human ORs can cause changes in OR
223 function when tested *in vitro*^{5,41-43}. Loss-of-function variants of ORs are often associated with
224 reduced odor sensation to their ligands, suggesting direct connections between OR activation
225 and odor perception⁴⁴. Consistent with the role of OR2T family members in sulfur odor
226 perception, genetic variation of OR2T6 is associated with liking onions, whose key aroma

227 components are sulfur-containing volatiles⁴⁵. Additionally, mouse homologs of OR2T family
228 members are among the most significantly activated ORs by sulfur-containing odorants *in vivo*
229⁴⁶, supporting the notion that OR2T members are among the most potent ORs against the VSCs.

230 The binding of sulfur odorants with copper has been studied *in silico* using homology
231 models, which suggested that residues interact with the odorants^{28-30,34,35} (Extended data Fig.
232 6). Here, using AlphaFold structural models, we showed that specific residues within the
233 transmembrane domain 5 (C^{BW5.43} and M^{BW5.39}) are critical for OR2T1, OR2T6, and OR2T11
234 binding to hydrogen sulfide and methanethiol complexed with copper. Our models are
235 consistent with those of Haag et al.,³⁵ and Vihani et al.,⁴⁶ which noted the potential importance
236 of TM5 in copper-OR complex, notably by a^{5.39}MYxCC^{5.43} motif that is more prevalent in
237 sulfur-activated ORs⁴⁶. This motif is composed of sulfur-containing amino acids that can
238 coordinate copper and may be how many sulfur-specific ORs bind to sulfur odorants. Our
239 docking simulations also suggest that the β -ionone complex with these ORs occur at this same
240 location, preventing the effective binding of the sulfur agonists.

241 The use of OR antagonists in evaluating activation/inactivation of specific ORs in odor
242 perception has several advantages over genetic studies. Firstly, a given antagonist can block the
243 activation of multiple related ORs that may have redundant functions. In our study, β -ionone
244 antagonizes OR2T1 and OR2T11 that are activated by methanethiol. If these ORs have similar
245 roles in malodor sensation, it would be difficult to apply genetic methods due to the limited
246 effect size of each genetic variant without assessing a very large number of subjects, as done
247 with the UK biobank study⁴⁷. Secondly, we can test the same subject to evaluate the effects of
248 an antagonist (and a control) in odor perception, mitigating non-specific effects caused by

249 individuals' genetic backgrounds and other non-genetic variations. However, a given
250 antagonist for ORs may also act as an agonist for other ORs, creating a potential disadvantage
251 in distinguishing the effects of OR antagonisms from central processing in odor perception. We
252 addressed this challenge by selecting β -ionone, which shows wide variations in perceived odor
253 intensities among subjects^{44,48,49}. We demonstrated that intensity or pleasantness of β -ionone
254 has no correlation with odor suppressive effects against methanethiol. Crucially, the malodor
255 blocking effect was more effective when odorants were presented as a mixture in one nostril
256 than when they were presented separately in each nostril. This strongly supports our hypothesis
257 that β -ionone reduces methanethiol odor intensity and unpleasantness by antagonizing OR2T
258 family members activity.

259 Our study does not exclude the role of central processing in mixture suppression. In the case
260 of odor masking between 1-propanol and n-amyl, the masking effects were similar when two
261 substances were mixed or presented separately to the two nostrils simultaneously, indicating that
262 the central processing affects odor masking²³. In the present study, Iso E Super, which does not
263 potently block OR2T activities, also reduces malodor intensity albeit at lower efficacy,
264 suggesting a role of central processing in masking sulfur odors. Determining the relative roles of
265 antagonistic interactions between odorants and central processing in odor masking in different
266 odor mixtures is a critical step for the future.

267 Finally, our study highlights a potentially efficient strategy to identify novel deodorants via
268 *in vitro* screening of ORs. This strategy avoids biases, the limited throughput associated with
269 odor adaptation, and the fatigue of human sensory subjects during the initial screening phase.
270 Future studies should determine if this method is fruitful in discovering deodorants for various

271 environmental malodors.

272

273 **Acknowledgments**

274 We thank Priyanka Meesa, Emily Xu and Michael Sheyner for reading and editing the
275 manuscript.

276

277 **Author Contribution**

278 Y.F. conceived and designed the project. Y.F., M.A. and H.S. performed the ligand assay. R.E.
279 and T.T. conducted sensory evaluation test. C.D.M. performed ligand docking and binding
280 analysis, Y.F., H.M. and M.Y. carried out the analysis and wrote the paper with inputs from all
281 authors. Y.F., H.M. and Y.M. supervised the project.

282

283 **Funding**

284 This work was supported by grants from JSPS-KAKENHI (18K14060 and 20K15745 to Y.F.
285 20H02532 to M.Y.), JST ACT-X Grant Number JPMJAX201C and Program on Open
286 Innovation Platform with Enterprises, Research Institute and Academia JPMJOP183 to Y.F,
287 National Science Foundation grant 1555919 to HM, National Institute of Health grant
288 DC014423 and DC016224 to H.M., National Institute of Health grant K99DC018333 to
289 CADM.

290

291 **Declaration of interests**

292 Y.F., M.A., R.E. and T.T. filed patent applications relevant to this work. R.E. and T.T. are full-

293 time employee of S.T. Corporation. H.M. has received royalties from ChemCom, research
294 grants from Givaudan, and consultant fees from Kao Corporation. The remaining authors
295 declare no competing interests.

296

297 **Correspondence**

298 Correspondence should be addressed to Y.F., H.M. and M.Y.

299

300 **Methods**

301 **DNA and vector preparation.**

302 Open reading frames of human OR genes were subcloned into pCI (Promega, WI, USA)
303 with a Rho-tag (the sequence encoding the first 20 amino acids of rhodopsin) at the N terminal.
304 To generate mutants of ORs, DNA fragments of OR genes were amplified by PrimeStar MAX
305 polymerase (Takara bio, Shiga, Japan). The fragments were mixed and amplified by PCR reaction
306 to obtain full sequences. The plasmid for the expression of human ORs, RTP1S^{50,51}, and
307 pGlosensor F-22 (Promega) were amplified and purified by Nucleospin plasmid TF grade
308 (Takara bio, Shiga, Japan). All plasmid sequences were verified using Sanger sequencing (3100
309 Genetic Analyzer, Applied Biosystems).

310

311 **Cell culture.**

312 HEK293T and Hana 3A cells ⁵² were grown in Minimal Essential Medium (MEM)
313 containing 10% FBS (vol/vol) with penicillin-streptomycin and amphotericin B. Hana 3A cells
314 were authenticated using polymorphic short tandem repeat (STR) at the Duke DNA Analysis

315 Facility using GenePrint 10 (Promega) and shown to share profiles with the reference (ATCC).
316 All cell lines were incubated at 37°C, saturating humidity, and 5% CO₂. No mycoplasma
317 infection was detected in all cell cultures.

318

319 **Vapor Glosensor assay**

320 In the volatile sulfur detection test, Vapor Glosensor cAMP Assay (Promega) was used to
321 measure the changes in cAMP levels caused by receptor activation upon ligand binding¹¹.
322 Hana3A cells were plated on poly-D-Lysine coated 96-well plates. 18-24 hours after plating, cells
323 were transfected with 80 ng/well of plasmids encoding ORs, 5 ng/well of RTP1S⁵², and 10
324 ng/well of Glosensor plasmid (Promega). 18-24 hours later, the medium was replaced with 25
325 µL of HBSS (Gibco) containing 10 mM HEPES and 1 mM Glucose, followed by 25 µL of the
326 HBSS containing GloSensor cAMP Reagent (Promega). Plates were kept in a dark place at room
327 temperature for two hours to equilibrate cells with the reagent. The test plate was inserted into
328 the plate reader. The luminescence derived from basal activity in each ORs was measured. Before
329 odor stimulation of the cells expressing individual ORs on testing 96 well plate by odorants, a 96
330 well plate put into the 5L PET film sampling bag (Flek-Sampler, Omi odor air service Co., Shiga,
331 Japan) with a small fan. After 5L of pure air gas was inserted into the bag containing the assay
332 plate, H₂S or CH₃SH gas was added into same bag to make the desired gas phase concentration.
333 Based on a previous report that an odor response of the heterologous cells expressing ORs is
334 more than 1000 times weaker than that of olfactory sensory neuron cells¹², the stimulation
335 concentration for 1st screening (7 ppm for CH₃SH and 41 ppm for H₂S) was set to 10,000 times
336 the human olfactory threshold concentration (0.00007 ppm for CH₃SH and 0.00041 ppm for

337 H₂S)⁵³. Concentration of VSCs in sampling bag was measured with the Gas detector tube system
338 and detector tubes (No.70L for CH₃SH and No.4LL for H₂S) (GASTEC Corporation, Kanagawa,
339 Japan). Then the assay plate was incubated in the bag for 10 minutes. Immediately, the test plate
340 was inserted in the plate reader GloMAX discover (Promega) to measure the luminescence by
341 VSC stimulation. The luminescence in each well was measured. Response was evaluated by the
342 fold change in luminescence value before and after odor stimulation.

343 When the screening and evaluating antagonist was conducted, before putting the assay plate
344 into the sampling bag, tested fragrance solutions were put into each well on the assay plate. When
345 evaluating the response to each fragrance against ORs, all luminescence values were divided by
346 the value obtained from the cells transfected with the empty vector at the same cycle. Multiple
347 comparisons were performed using one-way analysis of variance (ANOVA) followed by
348 Dunnett's test with the target group set to control condition.

349

350 **Docking**

351 Structures were downloaded from the Alphafold 2 database (<https://alphafold.ebi.ac.uk/>,
352 downloaded 02/17/2022)⁵⁴. The most variable parts of the receptor were mainly located at the
353 Nter (Fig S12). OR2T1 possesses an amino acid abnormally longer Nter loop than mammals OR
354 (Fig S12 and S13) that is modelled with low confidence by Alphafold. In consequence, we
355 decided to truncate the Nter parts of the models as indicated in Fig S13. The structures of OR2T1,
356 OR2T6, and OR2T11 are very close as the Root Mean Square Deviation (RMSD) between the
357 structures are very low (Fig S12). Odorant (hydrogen sulfide, methanethiol and β -ionone) and
358 copper SDF files were downloaded from Pubchem⁵⁵ and converted in pdb with Open Babel 2.3.2

359 on PyRx 0.8⁵⁶ and in pdbqt with Autodock Tools 1.5.7⁵⁷. The truncated Alfaphold models were
360 converted in pdbqt files and the grid for docking ligands and copper was generated with Autodock
361 Tools (Fig S14). Docking was realized with Vina 1.2.0^{58,59}. On a rigid receptor, 20 poses were
362 generated with an energy range of 15 kcal/mol and an exhaustiveness of 10. Results were
363 analyzed on Autodock Tools, and visualized on VMD 1.9.3⁶⁰ and UCSF Chimera 1.15⁶¹.

364

365 **Sensory Evaluation test**

366 All procedures involving human subjects were approved by the ethics committee of ST
367 Corporation. All subjects gave informed consent to participate. A filter paper placed in a beaker
368 was impregnated with 1g of undiluted solution of fragrances. The beaker was placed in a 10L
369 sampling bag filled with non-odor pure air gas filtered through silica and activated charcoal.
370 The scented air was adjusted by allowing the bag to stand overnight at room temperature. A
371 new 3L sampling bag was willed with pure air gas. Then, 200ml of the scented air and 0.4 mL
372 of 2% CH₃SH gas (final concentration of 0.3 ppm) were injected into the bag. In the same
373 process each fragrance and CH₃SH gas alone were adjusted. Each odor bag was prepared for
374 the whole nose test and single-nostril test (Extended data Fig. 10). Subjects evaluated the total
375 intensity, malodor intensity and pleasantness against each condition. The example of answer
376 sheet shown in Extended data Fig. 10 was used for the evaluation. In order to clarify the
377 evaluation criteria, a non-blind test was conducted for Methanthiol alone and the other test in
378 the blind condition. In the test for β -ionone and Iso E Super, panelists (n=20) were divided into
379 two, and the order of the scents was changed for each. No grouping is performed for sensory
380 evaluation using other fragrances. The panelists were men and women in their 20s and 30s.

381 Detailed data of each panelist was also shown in Supplementary Data. The panelists evaluated
382 the degree of pleasant/unpleasant, the intensity of malodor, and the intensity of total odor.
383 Single nostril evaluation tests were performed in non-blind condition against the control bag
384 containing only pure air and the other test in the blind condition. Panelists were instructed to
385 sniff their hands and arms and reset their noses between samples. Nonparametric multiple
386 comparisons were performed using one-way analysis of variance (ANOVA) following Dunn's
387 or Friedman's multiple comparisons test using the GraphPad Prism. Correlation values were
388 also calculated by nonparametric Spearman correction test.

389

390 **Statistical analysis.**

391 Multiple comparisons were performed using one-way analysis of variance (ANOVA)
392 using the GraphPad Prism. Analysis methods for each data were also described in each methods
393 and figure legends.

394

395 **Data availability**

396 All relevant data are available within the manuscript and its supplementary information or
397 from the authors upon reasonable request.

398

399 **References**

- 400 1 Buck, L. & Axel, R. A novel multigene family may encode odorant receptors: a
401 molecular basis for odor recognition. *Cell* **65**, 175-187, doi:10.1016/0092-
402 8674(91)90418-x (1991).
- 403 2 Niimura, Y., Matsui, A. & Touhara, K. Extreme expansion of the olfactory receptor gene

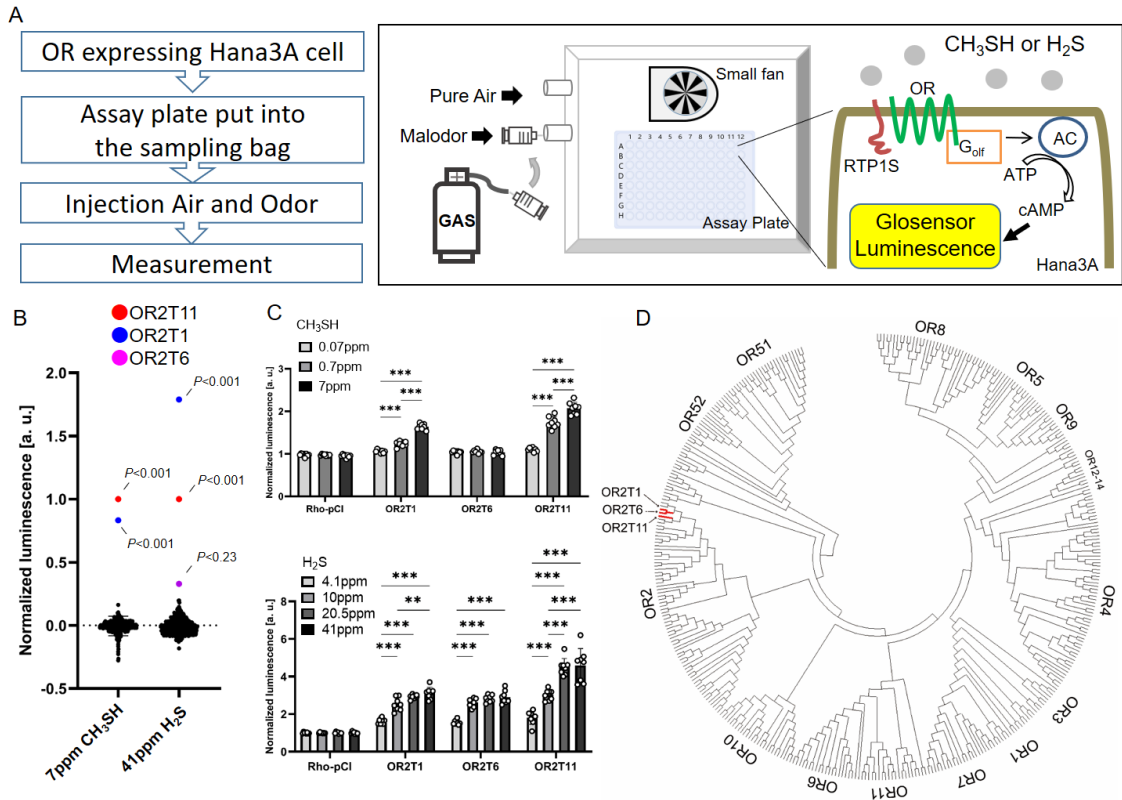
- 404 repertoire in African elephants and evolutionary dynamics of orthologous gene groups
405 in 13 placental mammals. *Genome Res* **24**, 1485-1496, doi:10.1101/gr.169532.113
406 (2014).
- 407 3 Adipietro, K. A., Mainland, J. D. & Matsunami, H. Functional evolution of mammalian
408 odorant receptors. *PLoS Genet* **8**, e1002821, doi:10.1371/journal.pgen.1002821
409 (2012).
- 410 4 Malnic, B., Godfrey, P. A. & Buck, L. B. The human olfactory receptor gene family.
411 *Proc Natl Acad Sci U S A* **101**, 2584-2589, doi:10.1073/pnas.0307882100 (2004).
- 412 5 Trimmer, C. *et al.* Genetic variation across the human olfactory receptor repertoire
413 alters odor perception. *Proc Natl Acad Sci U S A* **116**, 9475-9480,
414 doi:10.1073/pnas.1804106115 (2019).
- 415 6 Serizawa, S., Miyamichi, K. & Sakano, H. One neuron-one receptor rule in the mouse
416 olfactory system. *Trends Genet* **20**, 648-653, doi:10.1016/j.tig.2004.09.006 (2004).
- 417 7 Ferreira, T. *et al.* Silencing of odorant receptor genes by G protein betagamma signaling
418 ensures the expression of one odorant receptor per olfactory sensory neuron. *Neuron*
419 **81**, 847-859, doi:10.1016/j.neuron.2014.01.001 (2014).
- 420 8 Saito, H., Chi, Q., Zhuang, H., Matsunami, H. & Mainland, J. D. Odor coding by a
421 Mammalian receptor repertoire. *Sci Signal* **2**, ra9, doi:10.1126/scisignal.2000016
422 (2009).
- 423 9 Nara, K., Saraiva, L. R., Ye, X. & Buck, L. B. A large-scale analysis of odor coding in the
424 olfactory epithelium. *J Neurosci* **31**, 9179-9191, doi:10.1523/JNEUROSCI.1282-
425 11.2011 (2011).
- 426 10 Saraiva, L. R. *et al.* Combinatorial effects of odorants on mouse behavior. *Proc Natl*
427 *Acad Sci U S A* **113**, E3300-3306, doi:10.1073/pnas.1605973113 (2016).
- 428 11 Kida, H. *et al.* Vapor detection and discrimination with a panel of odorant receptors.
429 *Nat Commun* **9**, 4556, doi:10.1038/s41467-018-06806-w (2018).
- 430 12 Oka, Y., Omura, M., Kataoka, H. & Touhara, K. Olfactory receptor antagonism between
431 odorants. *EMBO J* **23**, 120-126, doi:10.1038/sj.emboj.7600032 (2004).
- 432 13 Liu, M. T. *et al.* Carbon chain shape selectivity by the mouse olfactory receptor OR-I7.
433 *Org Biomol Chem* **16**, 2541-2548, doi:10.1039/C8OB00205C (2018).
- 434 14 Singh, V., Murphy, N. R., Balasubramanian, V. & Mainland, J. D. Competitive binding
435 predicts nonlinear responses of olfactory receptors to complex mixtures. *Proc Natl Acad*
436 *Sci U S A* **116**, 9598-9603, doi:10.1073/pnas.1813230116 (2019).

- 437 15 Xu, L. *et al.* Widespread receptor-driven modulation in peripheral olfactory coding.
438 *Science* **368**, doi:10.1126/science.aaz5390 (2020).
- 439 16 Inagaki, S., Iwata, R., Iwamoto, M. & Imai, T. Widespread Inhibition, Antagonism, and
440 Synergy in Mouse Olfactory Sensory Neurons In Vivo. *Cell Rep* **31**, 107814,
441 doi:10.1016/j.celrep.2020.107814 (2020).
- 442 17 Pfister, P. *et al.* Odorant Receptor Inhibition Is Fundamental to Odor Encoding. *Curr*
443 *Biol* **30**, 2574-2587 e2576, doi:10.1016/j.cub.2020.04.086 (2020).
- 444 18 de March, C. A. *et al.* Modulation of the combinatorial code of odorant receptor
445 response patterns in odorant mixtures. *Mol Cell Neurosci* **104**, 103469,
446 doi:10.1016/j.mcn.2020.103469 (2020).
- 447 19 Reisert, J. Origin of basal activity in mammalian olfactory receptor neurons. *J Gen*
448 *Physiol* **136**, 529-540, doi:10.1085/jgp.201010528 (2010).
- 449 20 Brodin, M., Laska, M. & Olsson, M. J. Odor interaction between Bourgeonal and its
450 antagonist undecanal. *Chem Senses* **34**, 625-630, doi:10.1093/chemse/bjp044 (2009).
- 451 21 Spehr, M. *et al.* Dual capacity of a human olfactory receptor. *Curr Biol* **14**, R832-833,
452 doi:10.1016/j.cub.2004.09.034 (2004).
- 453 22 Burger, J. L., Jeerage, K. M. & Bruno, T. J. Direct nuclear magnetic resonance
454 observation of odorant binding to mouse odorant receptor MOR244-3. *Anal Biochem*
455 **502**, 64-72, doi:10.1016/j.ab.2016.03.006 (2016).
- 456 23 Cain, W. S. Odor Intensity - Mixtures and Masking. *Chem Sens Flav* **1**, 339-352,
457 doi:DOI 10.1093/chemse/1.3.339 (1975).
- 458 24 Thomas-Danguin, T. *et al.* The perception of odor objects in everyday life: a review on
459 the processing of odor mixtures. *Frontiers in psychology* **5**, 504,
460 doi:10.3389/fpsyg.2014.00504 (2014).
- 461 25 Kurahashi, T., Lowe, G. & Gold, G. H. Suppression of odorant responses by odorants in
462 olfactory receptor cells. *Science* **265**, 118-120, doi:10.1126/science.8016645 (1994).
- 463 26 Wallrabenstein, I., Singer, M., Panten, J., Hatt, H. & Gisselmann, G. Timberol(R)
464 Inhibits TAAR5-Mediated Responses to Trimethylamine and Influences the Olfactory
465 Threshold in Humans. *PLoS One* **10**, e0144704, doi:10.1371/journal.pone.0144704
466 (2015).
- 467 27 de March, C. A., Fukutani, Y., Vihani, A., Kida, H. & Matsunami, H. Real-time In Vitro
468 Monitoring of Odorant Receptor Activation by an Odorant in the Vapor Phase. *J Vis*
469 *Exp*, doi:10.3791/59446 (2019).

- 470 28 Li, S. *et al.* Smelling Sulfur: Copper and Silver Regulate the Response of Human
471 Odorant Receptor OR2T11 to Low-Molecular-Weight Thiols. *J Am Chem Soc* **138**,
472 13281-13288, doi:10.1021/jacs.6b06983 (2016).
- 473 29 Block, E., Batista, V. S., Matsunami, H., Zhuang, H. & Ahmed, L. The role of metals in
474 mammalian olfaction of low molecular weight organosulfur compounds. *Nat Prod Rep*
475 **34**, 529-557, doi:10.1039/c7np00016b (2017).
- 476 30 Zhang, R. *et al.* A Multispecific Investigation of the Metal Effect in Mammalian
477 Odorant Receptors for Sulfur-Containing Compounds. *Chemical senses* **43**, 357-366,
478 doi:10.1093/chemse/bjy022 (2018).
- 479 31 Gautschi, M., Bajgrowicz, J. A. & Kraft, P. Fragrance chemistry - Milestones and
480 perspectives. *Chimia* **55**, 379-387 (2001).
- 481 32 Armanino, N. *et al.* What's Hot, What's Not: The Trends of the Past 20 Years in the
482 Chemistry of Odorants. *Angew Chem Int Ed Engl* **59**, 16310-16344,
483 doi:10.1002/anie.202005719 (2020).
- 484 33 Jumper, J. *et al.* Highly accurate protein structure prediction with AlphaFold. *Nature*
485 **596**, 583-589, doi:10.1038/s41586-021-03819-2 (2021).
- 486 34 Duan, X. *et al.* Crucial role of copper in detection of metal-coordinating odorants. *Proc*
487 *Natl Acad Sci U S A* **109**, 3492-3497, doi:10.1073/pnas.1111297109 (2012).
- 488 35 Haag, F. *et al.* Copper-mediated thiol potentiation and mutagenesis-guided modeling
489 suggest a highly conserved copper-binding motif in human OR2M3. *Cell Mol Life Sci*,
490 doi:10.1007/s00018-019-03279-y (2019).
- 491 36 de March, C. A. *et al.* Conserved Residues Control Activation of Mammalian G Protein-
492 Coupled Odorant Receptors. *J Am Chem Soc* **137**, 8611-8616,
493 doi:10.1021/jacs.5b04659 (2015).
- 494 37 Wu, Y., Chen, K., Ye, Y., Zhang, T. & Zhou, W. Humans navigate with stereo olfaction.
495 *Proc Natl Acad Sci U S A* **117**, 16065-16071, doi:10.1073/pnas.2004642117 (2020).
- 496 38 Reddy, G., Zak, J. D., Vergassola, M. & Murthy, V. N. Antagonism in olfactory receptor
497 neurons and its implications for the perception of odor mixtures. *Elife* **7**,
498 doi:10.7554/eLife.34958 (2018).
- 499 39 Zak, J. D., Reddy, G., Vergassola, M. & Murthy, V. N. Antagonistic odor interactions in
500 olfactory sensory neurons are widespread in freely breathing mice. *Nat Commun* **11**,
501 3350, doi:10.1038/s41467-020-17124-5 (2020).
- 502 40 Ishii, A. *et al.* Synergy and masking in odor mixtures: an electrophysiological study of

- 503 orthonasal vs. retronasal perception. *Chem Senses* **33**, 553-561,
504 doi:10.1093/chemse/bjn022 (2008).
- 505 41 Keller, A., Zhuang, H., Chi, Q., Vosshall, L. B. & Matsunami, H. Genetic variation in a
506 human odorant receptor alters odour perception. *Nature* **449**, 468-472,
507 doi:10.1038/nature06162 (2007).
- 508 42 Mainland, J. D. *et al.* The missense of smell: functional variability in the human odorant
509 receptor repertoire. *Nat Neurosci* **17**, 114-120, doi:10.1038/nn.3598 (2014).
- 510 43 McRae, J. F. *et al.* Genetic variation in the odorant receptor OR2J3 is associated with
511 the ability to detect the "grassy" smelling odor, cis-3-hexen-1-ol. *Chem Senses* **37**, 585-
512 593, doi:10.1093/chemse/bjs049 (2012).
- 513 44 Jaeger, S. R. *et al.* A Mendelian trait for olfactory sensitivity affects odor experience and
514 food selection. *Curr Biol* **23**, 1601-1605, doi:10.1016/j.cub.2013.07.030 (2013).
- 515 45 May-Wilson, S. *et al.* Large-scale genome-wide association study of food liking reveals
516 genetic determinants and genetic correlations with distinct neurophysiological traits.
517 *bioRxiv*, 2021.2007.2028.454120, doi:10.1101/2021.07.28.454120 (2021).
- 518 46 Vihani, A. *et al.* Encoding of odors by mammalian olfactory receptors. *bioRxiv*,
519 2021.2012.2027.474279, doi:10.1101/2021.12.27.474279 (2021).
- 520 47 Sanchez-Roige, S., Gray, J. C., MacKillop, J., Chen, C. H. & Palmer, A. A. The genetics
521 of human personality. *Genes Brain Behav* **17**, e12439, doi:10.1111/gbb.12439 (2018).
- 522 48 Plotto, A., Barnes, K. W. & Goodner, K. L. Specific Anosmia Observed for β -Ionone,
523 but not for α -Ionone: Significance for Flavor Research. *J. Food Sci.* **71**, S401- S406
524 (2006).
- 525 49 McRae, J. F. *et al.* Identification of regions associated with variation in sensitivity to
526 food-related odors in the human genome. *Curr Biol* **23**, 1596-1600,
527 doi:10.1016/j.cub.2013.07.031 (2013).
- 528 50 Zhuang, H. & Matsunami, H. Synergism of accessory factors in functional expression of
529 mammalian odorant receptors. *J Biol Chem* **282**, 15284-15293,
530 doi:10.1074/jbc.M700386200 (2007).
- 531 51 Fukutani, Y. *et al.* The N-terminal region of RTP1S plays important roles in dimer
532 formation and odorant receptor-trafficking. *J Biol Chem* **294**, 14661-14673,
533 doi:10.1074/jbc.RA118.007110 (2019).
- 534 52 Saito, H., Kubota, M., Roberts, R. W., Chi, Q. & Matsunami, H. RTP family members
535 induce functional expression of mammalian odorant receptors. *Cell* **119**, 679-691,

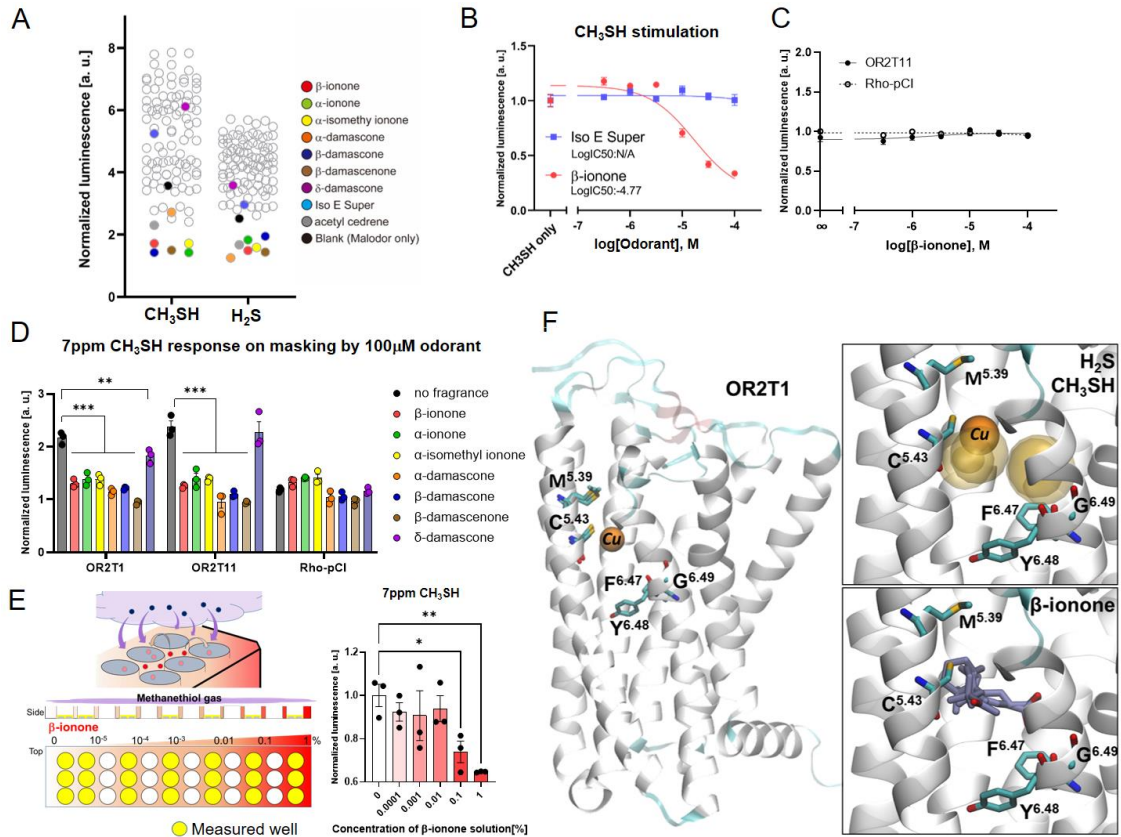
536 doi:10.1016/j.cell.2004.11.021 (2004).
537 53 Yoshio, Y. & Nagata, E.
538 54 Tunyasuvunakool, K. *et al.* Highly accurate protein structure prediction for the human
539 proteome. *Nature* **596**, 590-596, doi:10.1038/s41586-021-03828-1 (2021).
540 55 Kim, S. *et al.* PubChem in 2021: new data content and improved web interfaces.
541 *Nucleic Acids Res* **49**, D1388-D1395, doi:10.1093/nar/gkaa971 (2021).
542 56 O'Boyle, N. M. *et al.* Open Babel: An open chemical toolbox. *J Cheminform* **3**, 33,
543 doi:10.1186/1758-2946-3-33 (2011).
544 57 Goodsell, D. S. & Olson, A. J. Automated docking of substrates to proteins by simulated
545 annealing. *Proteins* **8**, 195-202, doi:10.1002/prot.340080302 (1990).
546 58 Eberhardt, J., Santos-Martins, D., Tillack, A. F. & Forli, S. AutoDock Vina 1.2.0: New
547 Docking Methods, Expanded Force Field, and Python Bindings. *J Chem Inf Model* **61**,
548 3891-3898, doi:10.1021/acs.jcim.1c00203 (2021).
549 59 Trott, O. & Olson, A. J. AutoDock Vina: improving the speed and accuracy of docking
550 with a new scoring function, efficient optimization, and multithreading. *J Comput*
551 *Chem* **31**, 455-461, doi:10.1002/jcc.21334 (2010).
552 60 Humphrey, W., Dalke, A. & Schulten, K. VMD: visual molecular dynamics. *J Mol Graph*
553 **14**, 33-38, 27-38, doi:10.1016/0263-7855(96)00018-5 (1996).
554 61 Pettersen, E. F. *et al.* UCSF Chimera--a visualization system for exploratory research
555 and analysis. *J Comput Chem* **25**, 1605-1612, doi:10.1002/jcc.20084 (2004).
556



557
558
559
560
561
562
563
564
565
566
567
568
569

Figure 1 | Screening of human ORs responding volatile sulfur compounds.

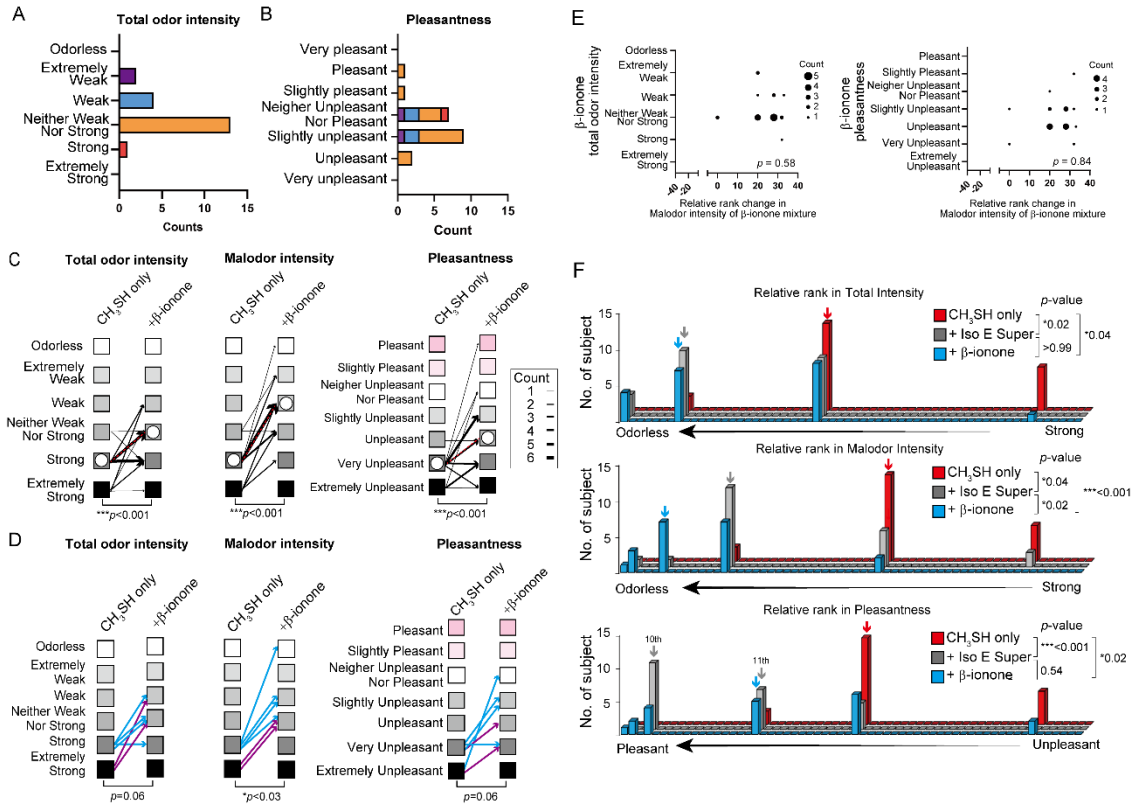
A) Schematic representation of the vapor stimulation assay with the OR signal transduction pathway. AC; adenylyl cyclase, ATP; adenosine triphosphate, cAMP; cyclic adenosine monophosphate, RTP1S; receptor transporting protein 1 short. B) Response of 359 unique human ORs against 7 ppm CH₃SH and 41 ppm H₂S in vapor phase. Multiple comparisons were performed using one-way analysis of variance (ANOVA) followed by Dunnett's Test. C) Vapor dose response analysis of identified human ORs. The normalized luminescence value indicates the S/N ratio before and after stimulation of CH₃SH or H₂S. Multiple comparisons were performed using one-way analysis of variance (ANOVA) followed by Dunnett's Test (*p<0.05, **p<0.01, ***p<0.001). D) Similarity of OR2T1, OR2T6 and OR2T11 in phylogenetic tree of human ORs.



570
571
572
573
574
575
576
577
578
579
580
581
582
583
584
585
586
587
588
589
590

Figure 2 | Antagonists of VSC responding human ORs

A) Screening for 100 odorants that inhibit the VSC response of OR2T11. B) Dose response inhibition of β -ionone (red) and Iso E Super (blue) against OR2T11 with the vapor concentration of CH₃SH held constant at 7ppm. IC₅₀ value was calculated using Graph pad Prism software. C) Dose–response curves of OR2T11 against β -ionone. D) Antagonistic effect of damascone & ionone analogs. 7ppm CH₃SH stimulation of human OR2T1 and OR2T11 masked by 100 μ M odorants. Multiple comparisons were performed using one-way analysis of variance (ANOVA) followed by Dunnett's multiple comparison test (** p <0.01, *** p <0.001). E) Inhibitory effect in vapor phase. Soon after adding 25 μ L of β -ionone (red) solution between the wells of the 96-well plate, OR2T11 expressing cells were quickly stimulated by CH₃SH gas (blue). The normalized luminescence value indicates the S/N ratio before and after stimulation of CH₃SH. Multiple comparisons were performed using one-way analysis of variance (ANOVA) followed by Dunnett's Test (* p <0.05, ** p <0.01) F). Left. View of the OR2T1, 2T6 and 2T11 AlphaFold models. Residues M^{BW}5.39 and C^{BW}5.43 are represented for the three ORs while the rest of the structure is only shown for OR2T1 for clarity. The docked copper is shown in orange Van der Waals volume. The toggle switch of mammals ORs, the FYG motif at positions F^{BW}6.47 to G^{BW}6.49, is also developed and serves as reference for the bottom of the odorant binding site. Right. Top. All the docking position of H₂S and methanethiol in the binding cavity of the three OR2T are represented in transparent volume. Bottom. The docking position of β -ionone in the three OR2T binding cavity are represented in blue licorice.



591

592

Figure 3 | β-ionone changes odor perception against VSC

593 Human Sensory evaluation test against CH₃SH gas containing β-ionone, an effective antagonist. A)

594 Odor intensity value of β-ionone evaluated by 20 subjects. B) Pleasantness value of β-ionone. Color

595 matched the odor intensity score of each subjects representing in Fig 3A. Comparison test was

596 performed using the non-parametric Wilcoxon test Test (***)*p*<0.001). C) Results of evaluation test

597 Total odor intensity Malodor intensity and Pleasantness. Line thickness: The number of subjects who

598 made the same evaluation transition in mixture gas. Median showed the white circle in each condition.

599 D) Results of evaluation test limited to subjects who is difficult to feel β-ionone, Blue :Weak,

600 purple:Extremely weak in Fig. 3A. Each line indicates one subject. Comparison test was performed

601 using the non-parametric Wilcoxon test Test (**p*<0.05). E) Correlation analysis between relative rank

602 change in malodor intensity by mixing with β-ionone (X-axis) and total odor intensity (Upper) or

603 pleasantness (Lower) score of the β-ionone (Y-axis). Plot size: number. Correlation values were

604 calculated by nonparametric Spearman correction test. F) Relative rank in Total intensity, malodor

605 intensity and pleasantness. Median showed the color arrows in each condition. Both are shown when

606 the 10th and 11th are different. Multiple comparison test was conducted using nonparametric

607 Friedman's test (**p*<0.05)

608



609
610

Figure 4 | Single nostril sensory evaluation

A) Schematic image of single nostril stimulation in human sensory evaluation test and test odor combinations. B) Test score of whether the malodor comes from the left or right direction in nostril stimulation. Subjects presented the direction they felt strongly. C) Results of evaluation test malodor intensity and total intensity for β -ionone single condition. Comparison test was performed using the non-parametric Wilcoxon test. D) Results of evaluation test for Odor intensity, Malodor intensity and Pleasantness, Center panel: CH₃SH only, Left panel: mixture gas of CH₃SH and β -ionone, Right panel: single nostril stimulation by CH₃SH and β -ionone separately. Each color indicated the score of one subject. Median showed the white circle in each condition. Nonparametric multiple comparisons against mean values were performed using one-way analysis of variance (ANOVA) followed by Dunn's multiple comparisons test (* $p<0.05$). E) Comparison of which of the stimulus conditions gave the better score. Odor intensity (Left), Malodor intensity (middle) and Pleasantness (Right). F) Relative rank in odor intensity (Upper), malodor intensity (middle) and pleasantness (Lower). Median

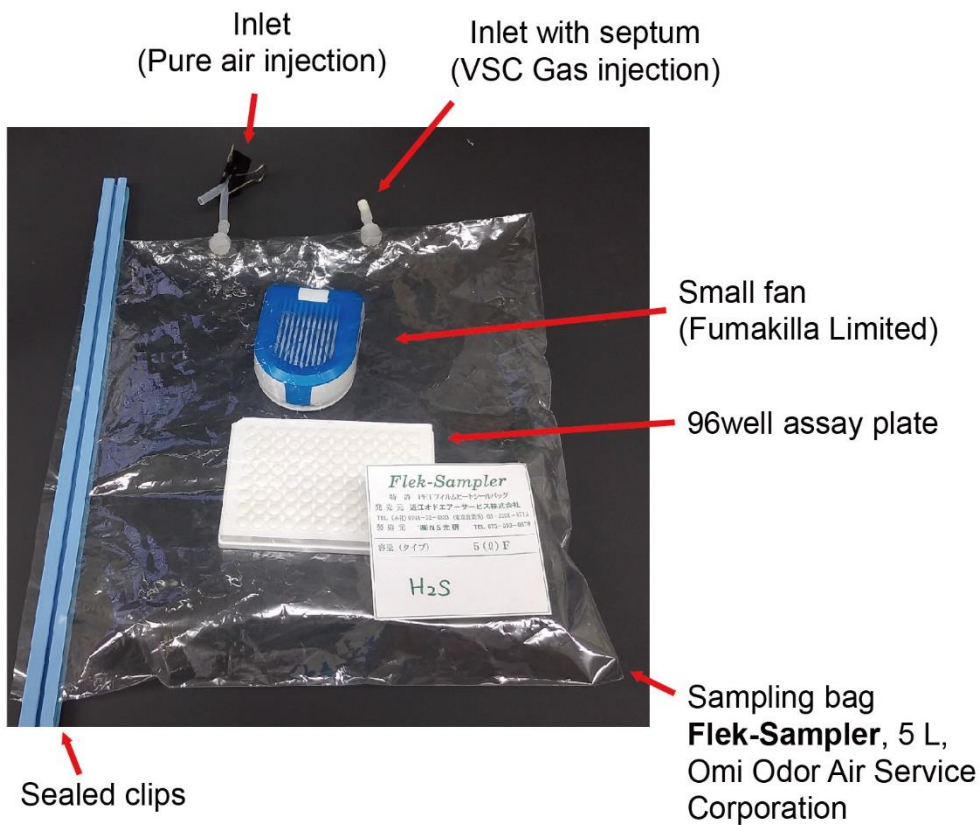
624 showed the color arrows in each condition. Both are shown when the 7th and 8th are different.
625 Multiple comparison test was conducted using nonparametric Friedman's test (* $p < 0.05$)

626

627 **Supplementary Figures**

628

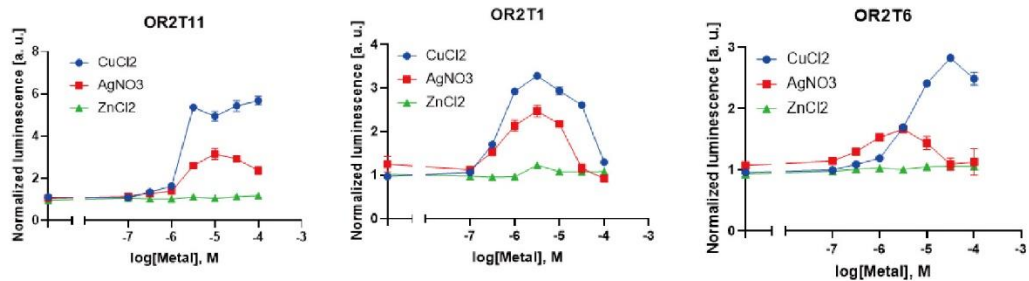
bioRxiv preprint doi: <https://doi.org/10.1101/2022.08.02.502184>; this version posted August 3, 2022. The copyright holder for this preprint (which was not certified by peer review) is the author/funder, who has granted bioRxiv a license to display the preprint in perpetuity. It is made available under a [CC-BY-NC-ND 4.0 International license](#).



Extended data Figure 1 | Photo image of the vapor stimulation assay with the cell culturing 96 well assay plate and the small fan in the sampling bag

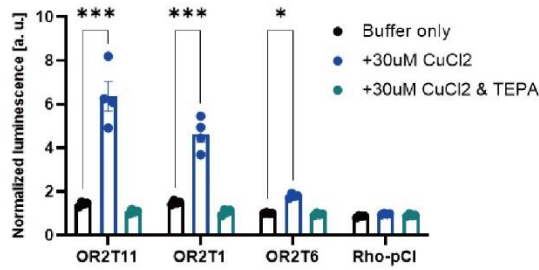
A

20ppm H₂S stimulation

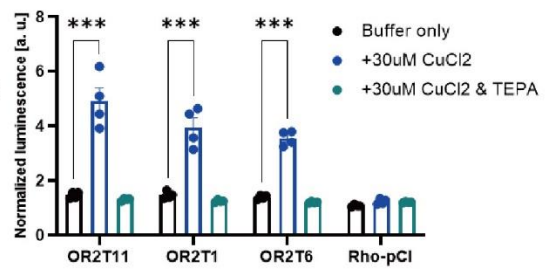


B

7ppm CH₃SH stimulation

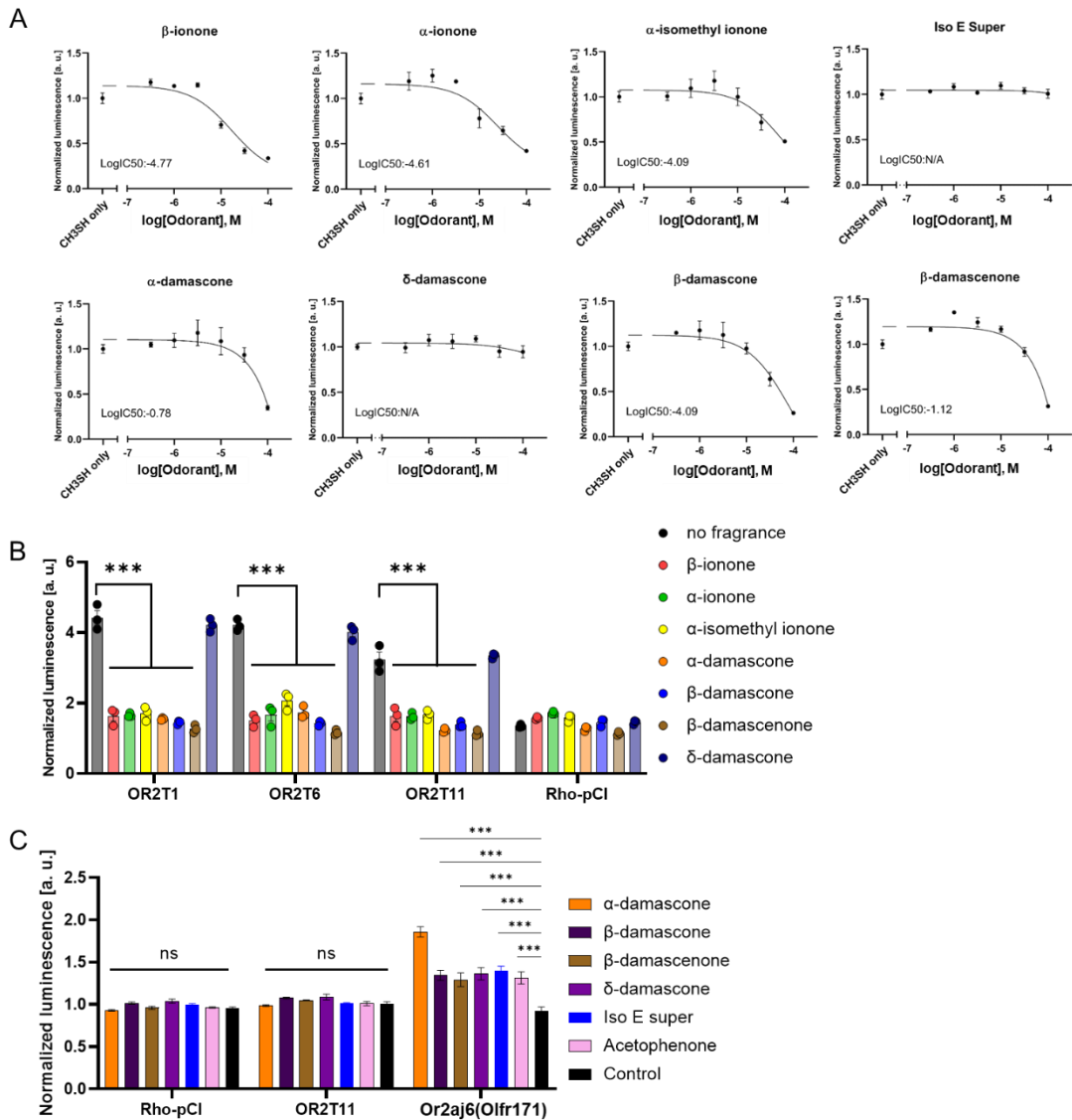


41ppm H₂S stimulation



Extended data Figure 2 | VSC binding on odorant receptors via copper ions. A metal ion is essential for CH₃SH/H₂S responding ORs. A) Dose-response curves of 3 ORs against increasing concentrations of metals with the concentration of vapor H₂S constant at 20 ppm. B) Cu²⁺ Cheater TEPA diminished the response of ORs

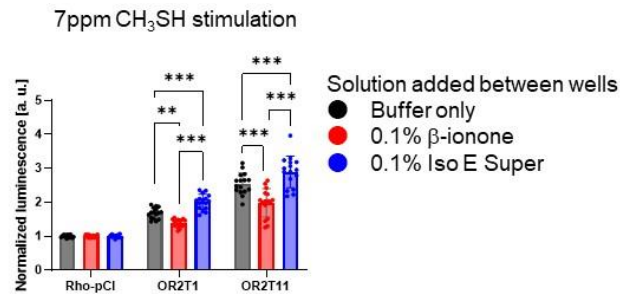
against both of H₂S and CH₃SH. The y-axis indicates normalized response ± s.e.m (n=3). Multiple comparisons were performed using one-way analysis of variance (ANOVA) followed by Dunnett's multiple comparison test (**p*<0.05. ***p*<0.01, ****p*<0.001).



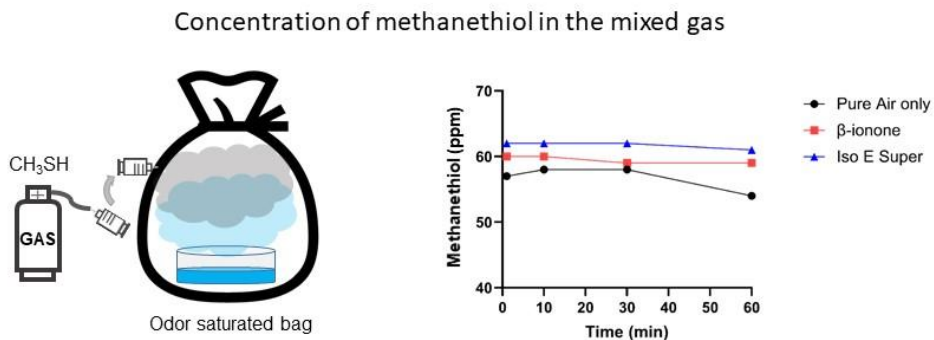
Extended data Figure 3 | Dose response analysis of candidate antagonists. A) Dose-response curves of OR2T11 against increasing concentrations of ionones and damascones, with the vapor concentration of CH₃SH held constant at 7 ppm. IC₅₀ value was calculated using Graph pad Prism software. B) Antagonistic effect of damascone & ionone analogs. 41 ppm H₂S stimulation on human OR2T1, OR2T6 and OR2T11 were masked by 100 μ M fragrance compounds. Multiple comparisons were performed using one-way

analysis of variance (ANOVA) followed by Dunnett's multiple comparison test (***p*<0.001). C) Inhibitor odorants did not cause adverse effects on the assay system. OR2T11 and mouse Or2aj6 (Olf171) (damascones responding receptor) expressing cells were stimulated by 100 μ M odorants and Glosensor buffer without any odorant as a negative control. Error bars indicate s.e.m (n=3) Multiple comparisons were performed using one-way ANOVA followed by Dunnett's test (***p*<0.001).

A



B



Extended data Figure 4 | Inhibitory effects of β -ionone in the vapor phase A) Inhibitory effect on vapor phase mixing β -ionone or Iso E super. Soon after adding 25 μ L of β -ionone or Iso E Super solution between the wells of the 96-well plate, OR expressing cells was quickly stimulated by 7ppm CH₃SH gas for 10 min. The normalized luminescence value indicates the S/N ratio before and after stimulation of CH₃SH. Multiple comparisons were performed using one-way analysis of

variance (ANOVA) followed by Dunnett's Test (* p <0.05. ** p <0.01)

B) Concentration of methanethiol in the sampling bag containing β -ionone or Iso E Super. methanethiol gas was injected into the saturated gas phase of β -ionone or Iso E Super in the sampling bag. Concentration of methanethiol in sampling bag was measured with the Gas detector tube system and detector tube No.70L for CH₃SH detection.

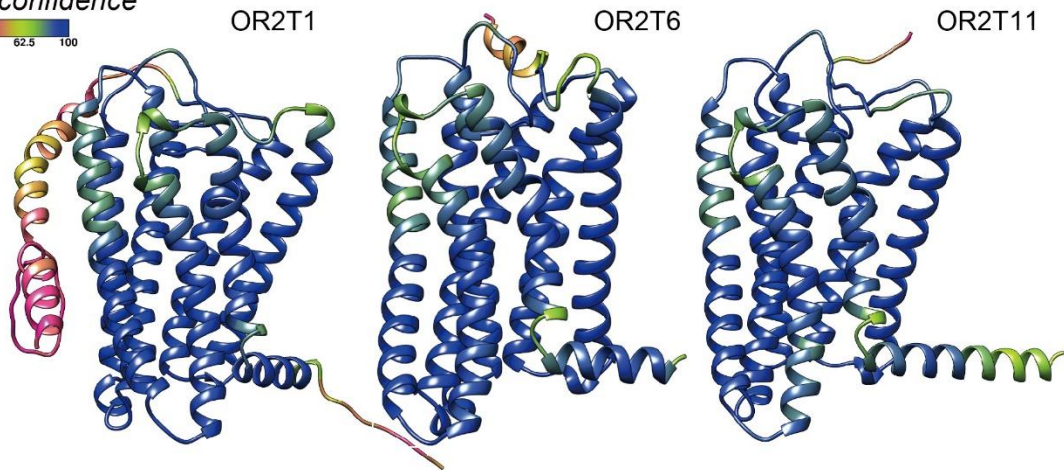
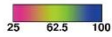
A



RMSD (Å)	OR2T1	OR2T6	OR2T11	OR1A1
OR2T1	-	0.76	0.83	6.46
OR2T6	0.76	-	0.83	6.42
OR2T11	0.83	0.83	-	6.41
OR1A1	6.46	6.42	6.41	-

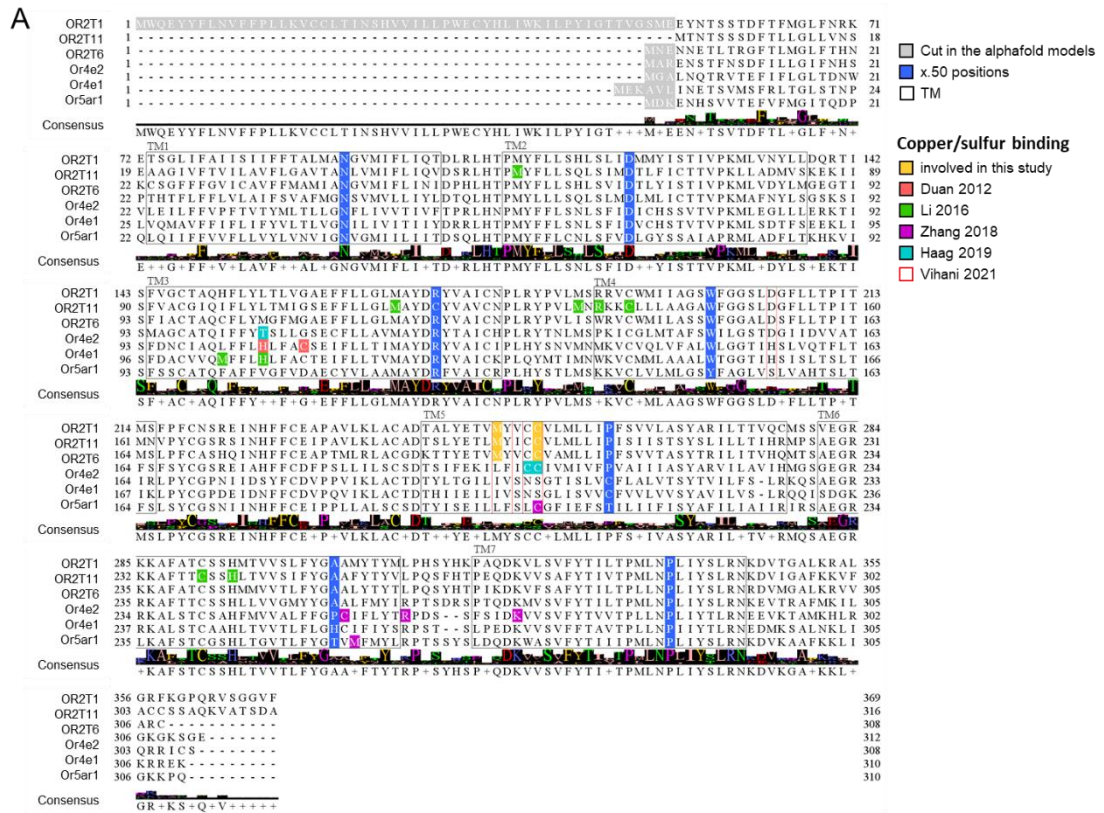
B

AF confidence

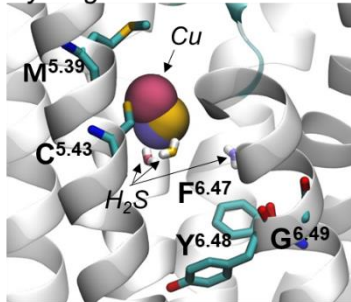


Extended data Figure 5 | 3D model of volatile sulfur responding ORs. A) Superimposition of the AlphaFold models of OR2T1, OR2T6 and OR2T11. RMSD

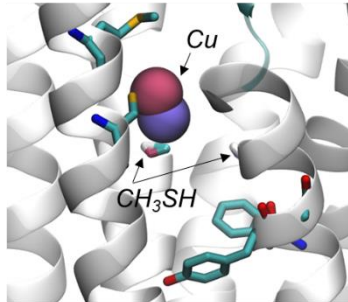
between the backbone of the structures is shown in a table. B) AlphaFold confidence score projected on the AlphaFold models of OR2T1, OR2T6 and OR2T11.



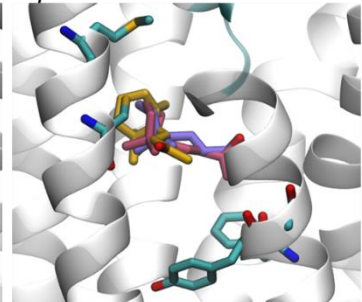
B hydrogen sulfide



C methanethiol



D β-ionone



E

affinity - Vina scores (kcal/mol)	OR2T1	OR2T11	OR2T6
Cu(Cl2)	-2.1	-2.1	-2
(Cu) H2S	-0.7	-0.4	-0.6
(Cu) methanethiol	-1.4	-0.9	-
β ionone	-0.7	-0.4	-5.6

F

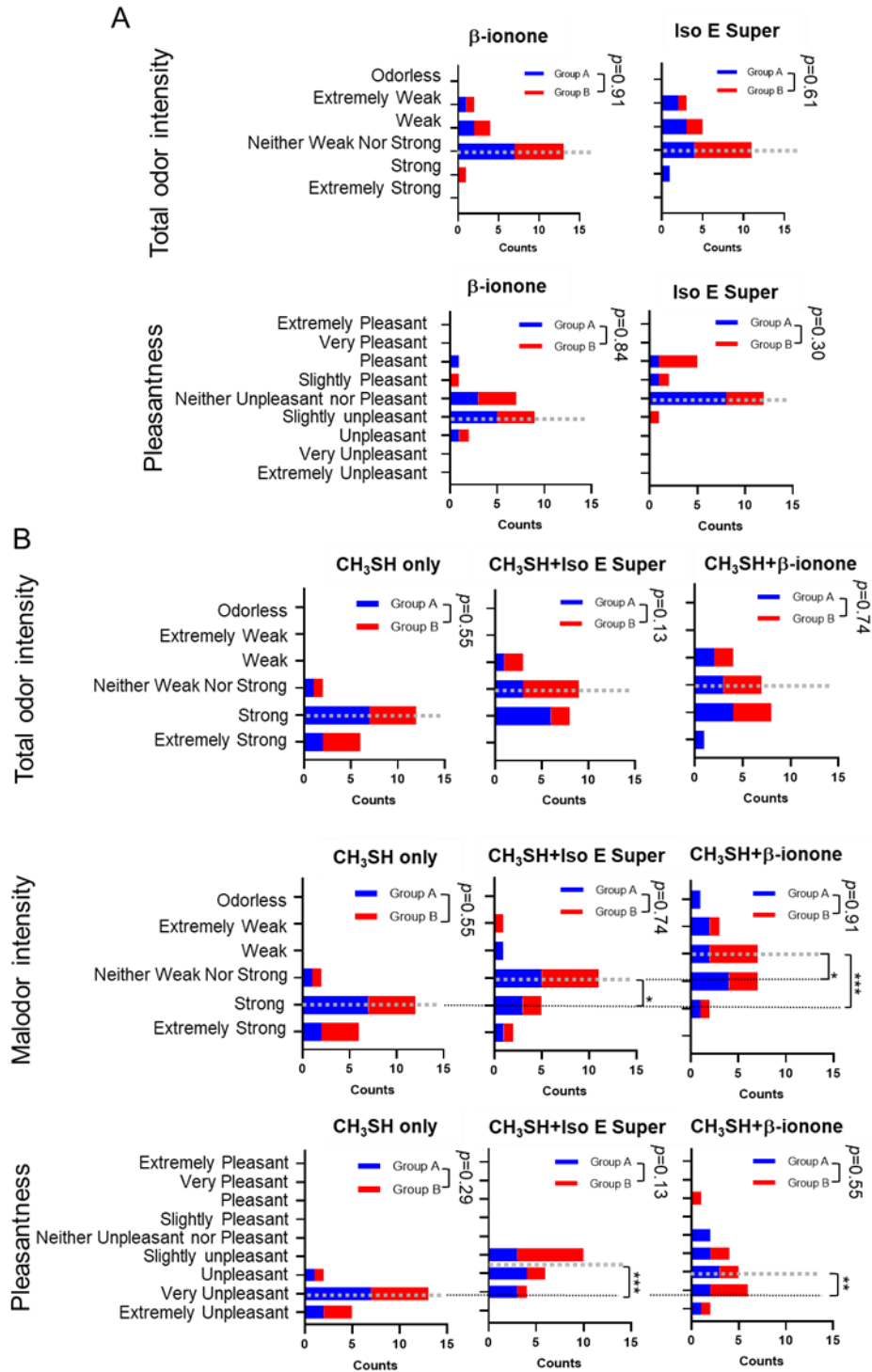
box Cu	OR2T1	OR2T11	OR2T6
dim-x	22	16	20
dim-y	20	14	14
dim-z	22	18	20
center-x	7.421	3.2	14.729
center-y	-3.701	13.392	-3.759
center-z	-5.42	-3.366	0.459

G

box ligands	OR2T1	OR2T11	OR2T6
dim-x	18	20	20
dim-y	14	18	18
dim-z	18	20	20
center-x	7.045	2.897	11.221
center-y	-6.741	9.751	-2.084
center-z	-3.07	-1.321	2.997

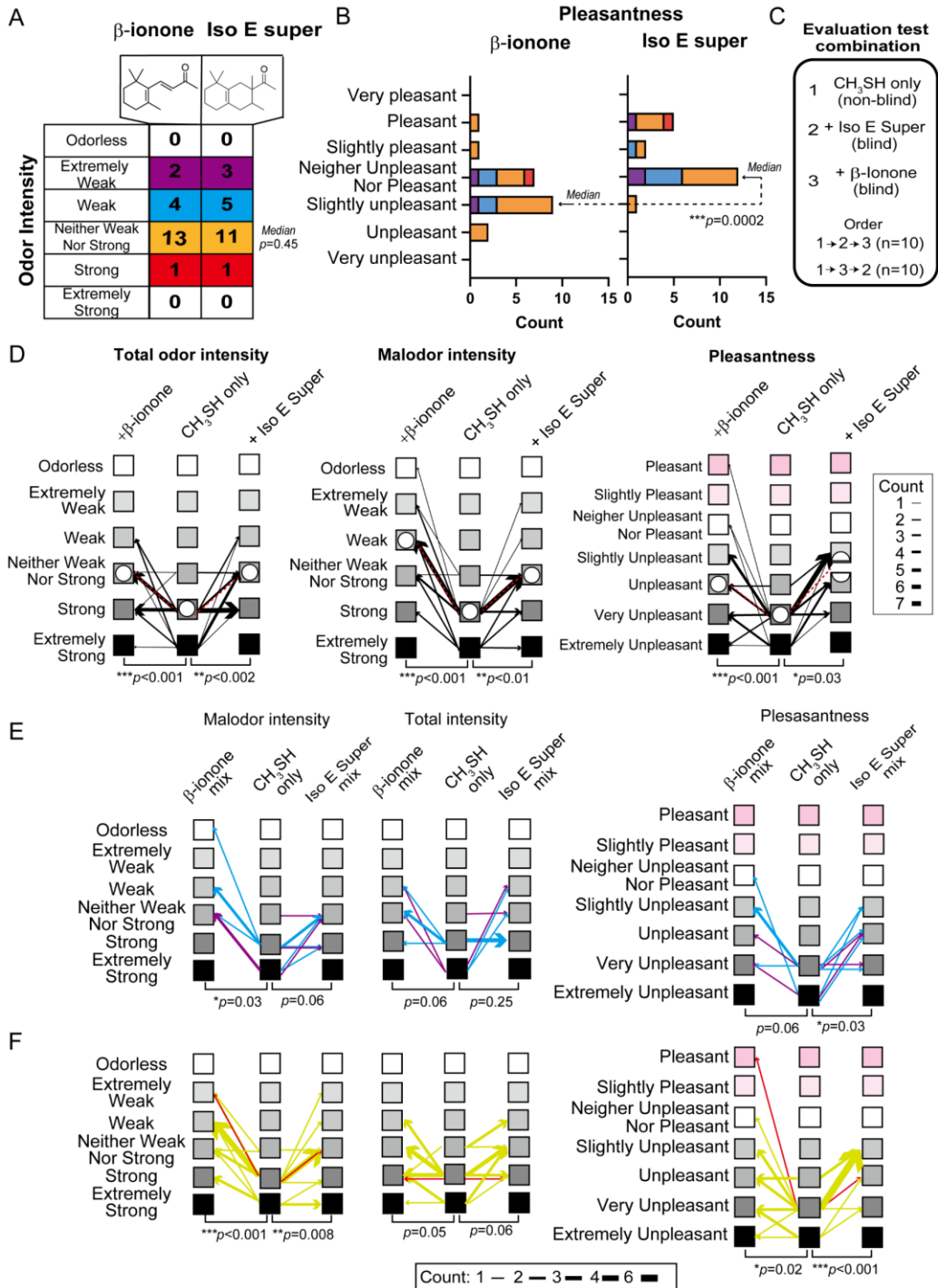
Extended data Figure 6 | Simulation analysis of inhibitory effects by β -ionone. A) Alignment of the sulfur responding OR studied in the literature. X.50 positions, TM domains as well as amino acids studied here and previously identified are highlighted. B-D) Docking results for H₂S (B), methanethiol (C) and β -ionone (D) for OR2T1 (purple), OR2T6 (yellow) and

OR2T11 (pink). Copper is represented in Van der Waals volume colored by OR while the ligand is represented in licorice with sulfur (H₂S and methanethiol) or carbon (β -ionone) atom colored by OR. E) Docking results by affinity represented by the Vina score. F) Box dimension and placement for copper docking. G) Box dimension and placement for ligand docking.



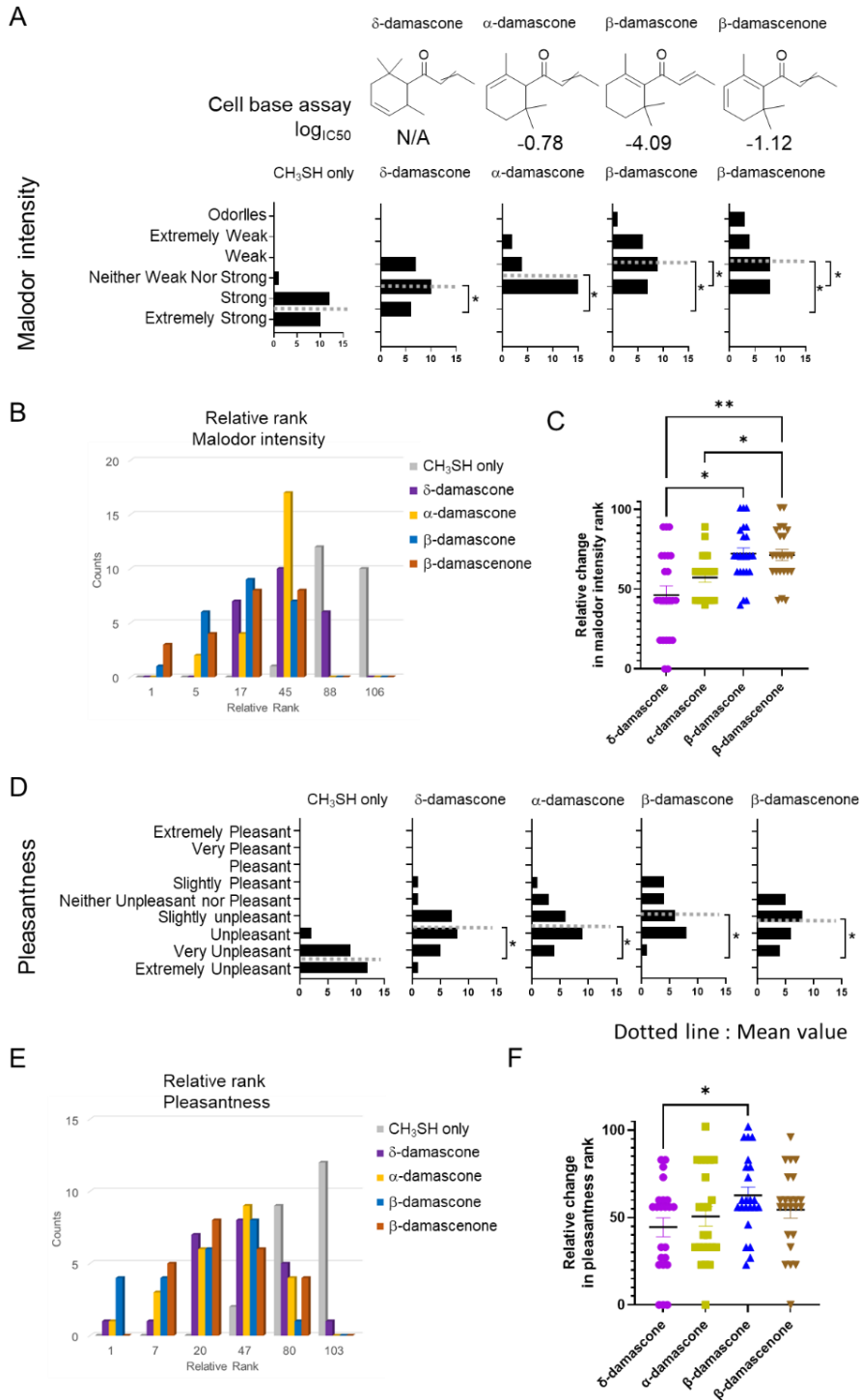
Extended data Figure 7 | Sensory evaluation test A) Score for β -ionone or Iso E Super. Red: Group A (n=10), Blue: Group B (n=10), Dot line: Median value. B) Score for methanethiol only, methanethiol and Iso E Super, and methyl methanethiol and β -ionone. Red: Group A (n=10), Blue: Group B (n=10), Dot line: Median value.

The significance analysis between Group A and B was performed using Mann-Whitney test. Nonparametric multiple comparisons among mixed gas were performed using one-way analysis of variance (ANOVA) followed by Dunn's multiple comparisons test (* p <0.05, ** p <0.01, *** p <0.001).



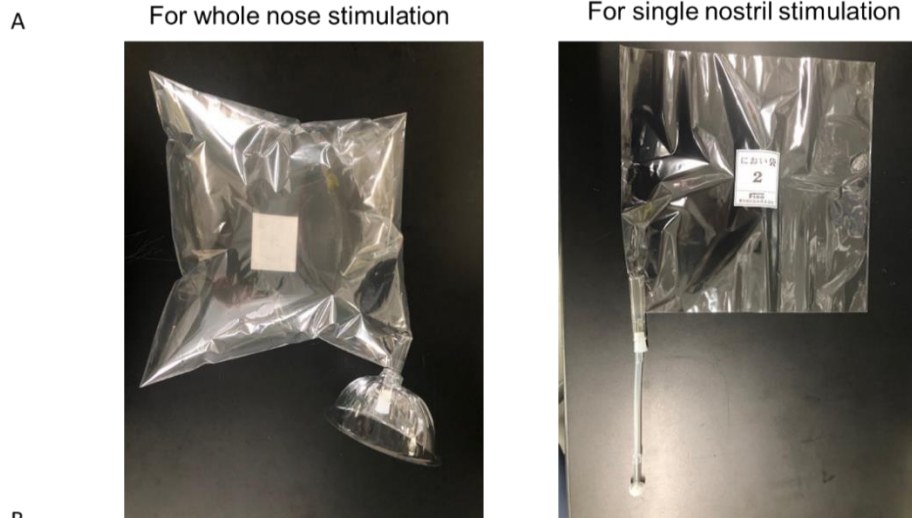
Extended data Figure 8 | Human Sensory evaluation test against CH₃SH gas containing β -ionone (an effective antagonist) or Iso E Super. A) Odor intensity value of β -ionone and Iso E Super evaluated by 20 subjects. B) Pleasantness value of β -ionone and Iso E Super. Color matched the odor intensity score of each subject representing in Extended Fig. 8A. Comparison test was performed using the non-parametric Wilcoxon test Test (** $p < 0.001$). C) Test odor combination and order in sensory evaluation test. D) Results of evaluation test Total odor intensity Malodor intensity and Pleasantness. Line thickness: The number of subjects

who made the same evaluation transition in mixture gas. Median showed the white circle in each condition. E and F) Results of evaluation test Total odor intensity Malodor intensity and Pleasantness when classified into Odor intensity scores of β -ionone or Iso E super. Color matched the odor intensity score of each subject representing in Extended Fig 8A (E: Extremely weak and Weak, F: Neither weak nor strong and Strong). Line thickness: The number of subjects who made the same evaluation transition in mixture gas. Comparison test was performed using the non-parametric Wilcoxon test Test.



Extended data Figure 9 | Damascones changes odor perception against VSC A and D) Sensory evaluation score for methanethiol only and mixture gas with damascones. A: Odor intensity, D: Pleasantness, Gray dot line: Mean value. Nonparametric multiple comparisons were performed using one-way analysis of

variance (ANOVA) followed by Dunn's multiple comparisons test ($*p<0.05$). B and E) Relative rank in malodor intensity and pleasantness, C and F) Relative rank change in malodor intensity (C) and pleasantness (F) Multiple comparison test was conducted using nonparametric Friedman's test ($*p<0.05$, $**p<0.01$).



B
Evaluation sheet in Japanese

	快・不快度						悪臭の強度					全体の強度							
	極端に不快	非常に不快	不快	やや不快	快	やや快	極端に不快	無臭	やや弱い	弱い	楽に感知できる	強い	強烈	無臭	やや弱い	弱い	楽に感知できる	強い	強烈
悪臭																			
A																			
B																			
C																			
D																			

Translation

	Pleasantness								Malodor intensity					Odor intensity							
	Extremely Unpleasant	Very Unpleasant	Unpleasant	Slightly unpleasant	Neither Unpleasant Nor Pleasant	Slightly Pleasant	Pleasant	Very Pleasant	Extremely Pleasant	Colorless	Extremely Weak	Weak	Neither Weak Nor Strong	Strong	Extremely Strong	Odorless	Extremely Weak	Weak	Neither Weak Nor Strong	Strong	Extremely Strong
Malodor																					
A																					
B																					
C																					
D																					

Extended data Figure 10 | Equipment for sensory evaluation test Left) Photographic image of the sampling bags used in sensory evaluation test. Upper) for whole nose stimulation (Results were shown in Figure 3), Lower) for single nostril stimulation test (Results were shown in Figure 4). Each has a suction

port of a suitable size. Right) Score sheet used in sensory evaluation tests. Upper: original score sheet written in Japanese. Lower: English translation version of original.